Acta Cryst. (1976). B**32**, 1767

The Tetragonal Crystal Structure of R_3Rh_2 Compounds with R=Gd, Tb, Dy, Ho, Er, Y

BY JEAN-MICHEL MOREAU,* DOMINIQUE PACCARD* AND ERWIN PARTHÉ

Laboratoire de Cristallographie aux Rayons X, Université de Genève, 24 *Quai Ernest-Ansermet, CH*-1211 *Geneva* 4, *Switzerland*

(*Received* 3 *December* 1975; *accepted* 30 *December* 1975)

Y_3Rh_2 crystallizes with a new tetragonal structure type. Space group *I*4/*mcm* (No. 140); $a = 11{\cdot}232$ (2), $c = 25{\cdot}16$ (1) Å, $Z = 28$, $D_x = 6{\cdot}92$ g cm^{-3}, F. W. 472·54, $F(000) = 5796$, μ(Mo $K\alpha$) = 460 cm^{-1}, $R = 0{\cdot}09$. Gd_3Rh_2, Tb_3Rh_2, Dy_3Rh_2, Ho_3Rh_2 and Er_3Rh_2 have the same structure as Y_3Rh_2. There are four different types of Rh-centred rare-earth polyhedra in the structure: a trigonal prism (as in R_3Rh and R_7Rh_3 with Fe_3C and Th_7Fe_3 types), a cube (as in RRh compounds with CsCl type), an Archimedian antiprism (as in R_5Rh_3 with Mn_5Si_3 type) and a truncated Archimedian antiprism (as in Pu_4CeCo_3 with W_5Si_3 type).

Introduction

Several new structures have been recently analysed in the binary systems of rare-earth elements and transition metals. For Co and Ni, when there is 50 or more at.% of rare earth in the alloy, most of the structures are characterized by a stacking of regular trigonal prisms, the rare-earth atoms being at the corners of the prism and the transition metal at its centre (see for example Moreau, Paccard & Parthé, 1974, 1976). It is of interest to verify whether the same structural features can be observed with Rh alloys of the same composition.

A survey of the intermediate phases in rare-earth Rh systems has been made by Ghassem & Raman (1973*b*). For compositions R_5Rh_3 and R_3Rh_2 five different structure types have been found of which only one has been solved and recognized to be the Mn_5Si_3 type. This study describes the structure determination of one of these unknown structure types which is denoted by Ghassem & Raman as the Er_3Rh_2 structure type.

Experimental

The alloys of this series R_3Rh_2 were made from commercially available elements of high purity: rare earth 99·9% and Rh 99·9%. The constituents were arc melted under an argon atmosphere. Single crystals of Y_3Rh_2 were directly isolated by mechanical fragmentation from the crushed melt.

Lattice constants (Table 1) and intensities of Y_3Rh_2 were measured with graphite-monochromated Mo $K\alpha$ radiation on a Philips PW 1100 computer-controlled four-circle goniometer in the θ–2θ scan mode. The intensities of 503 non-equivalent reflexions were recorded out to a limit of $\sin\theta/\lambda = 0{\cdot}5$ Å^{-1} and all were used in the structure determination. Because of the very irregular shape of the crystal, absorption corrections were made with the experimental method of Flack (1974, 1975). Examination of systematic absences indicated that *I*4/*mcm*, *I*4*cm* and $I\bar{4}c2$ were possible space groups.

Table 1. *Crystallographic data for* Y_3Rh_2

Space group	*I*4/*mcm* (No. 140)
a	11·232 (2) Å
c	25·16 (1)
Z	28
D_x	6·92 g cm^{-3}
μ(Mo $K\alpha$)	460 cm^{-1}

Structure determination

A comparison with the Pu_4CeCo_3 structure (Larson, Roof & Cromer, 1964) having the W_5Si_3 type (Aronsson, 1955) revealed a common space group *I*4/*mcm* and an almost identical a parameter, the only difference being the c parameter which is four times as large for Y_3Rh_2. Consequently an atomic model based on the W_5Si_3 type was considered and Fourier sections perpendicular to **c** were computed with observed Y_3Rh_2 amplitudes. It appeared that this model was roughly correct except for the $z=0$ and $z=\frac{1}{2}$ sections. Successive least-squares refinement followed by computation and examination of Fourier sections (X-RAY system, 1972) finally led to the correct model (Table 2). Relativistic Hartree–Fock scattering factors were used (Cromer & Mann, 1968). The final value of $R(=\sum|\Delta F|/\sum|F_o|)$ was 0·09 for 468 observed reflexions ($|F_o| > 2\sigma_F$).† A listing of the low-angle reflexions for Y_3Rh_2 with corresponding calculated intensities for X-ray powder diagram identification is given in Table 3 (Yvon, Jeitschko & Parthé, 1969).

* Centre Universitaire de Savoie, IUT Annecy et Laboratoire de Magnétisme, CNRS, Grenoble, France.

† A list of structure factors has been deposited with the British Library Lending Division as Supplementary Publication No. SUP 31586 (8 pp.). Copies may be obtained through The Executive Secretary, International Union of Crystallography, 13 White Friars, Chester CH1 1NZ, England.

Table 2. *Atomic parameters* ($\times 10^4$) *for* Y_3Rh_2 *with e.s.d.'s in parentheses*

The Debye–Waller factor is defined as $\exp[-8\pi^2U(\sin\theta/\lambda)^2]$. Space group *I*4/*mcm* (No. 140).

	Equipoint	x	y	z	U (Å^2) ($\times 10^2$)
Y(1)	32m	2042 (4)	757 (4)	712 (2)	1·9 (1)
Y(2)	32m	799 (4)	2113 (4)	1935 (2)	2·3 (1)
Y(3)	8h	3483 (6)	8483 (6)	0	2·3 (2)
Y(4)	8g	0	5000	1122 (4)	2·1 (2)
Y(5)	4b	0	5000	2500	2·2 (3)
Rh(1)	16l	3208 (4)	8208 (4)	1063 (2)	2·0 (2)
Rh(2)	16l	1553 (4)	6553 (4)	1885 (3)	2·7 (2)
Rh(3)	8h	960 (5)	5960 (5)	0	1·9 (2)
Rh(4)	8f	0	0	1335 (3)	1·3 (2)
Rh(5)	4c	0	0	0	1·3 (2)
Rh(6)	4a	0	0	2500	0·9 (2)

Table 3. *Calculated powder intensities and d spacing for* Y_3Rh_2 *from single-crystal data*

I_c is normalized to the strongest reflexion which is given an intensity of 1000. Lorentz and polarization corrections are made for a Guinier–de Wolff camera with Cu $K\alpha$ radiation ($\lambda = 1{\cdot}5418$ Å).

h	k	l	d-Value	Intensity
0	0	2	12·58	1·6
1	1	0	7·942	17·9
1	1	2	6·7158	41·3
0	0	4	6·2900	12·5
2	0	0	5·6160	8·9
2	0	2	5·1282	1·1
1	1	4	4·9309	12·0
2	1	1	4·9259	8·1
2	1	3	4·3093	2·9
0	0	6	4·1933	0·7
2	0	4	4·1892	52·2
2	2	0	3·9711	52·4
2	2	2	3·7869	0·0
1	1	6	3·7082	9·3
2	1	5	3·5550	119·8
3	1	0	3·5519	72·0
3	1	2	3·4182	9·0
2	0	6	3·3600	0·1
2	2	4	3·3579	20·8
0	0	8	3·1450	49·6
3	1	4	3·0928	12·2
3	2	1	3·0916	0·8
1	1	8	2·9241	44·2
2	1	7	2·9230	56·8
3	2	3	2·9202	212·3
2	2	6	2·8834	0·1
4	0	0	2·8080	1·5
2	0	8	2·7440	407·2
4	0	2	2·7406	22·0
3	1	6	2·7103	276·9
4	1	1	2·7083	431·1
3	2	5	2·6487	583·2
3	3	0	2·6474	213·3
4	1	3	2·5909	523·4
3	3	2	2·5907	0·4
4	0	4	2·5641	39·6
0	0	10	2·5160	241·2
4	2	0	2·5116	694·2
2	2	8	2·4655	756·7
4	2	2	2·4629	41·6
2	1	9	2·4427	223·8
3	3	4	2·4401	28·8
1	1	10	2·3985	67·4
4	1	5	2·3956	1000·0

Table 3 (*cont.*)

h	k	l	d-Value	Intensity
3	1	8	2·3546	245·8
3	2	7	2·3541	45·9
4	0	6	2·3332	108·5
4	2	4	2·3325	13·7
2	0	10	2·2961	79·1
3	3	6	2·2386	2·9
4	3	1	2·2375	13·9
5	1	0	2·2028	108·7
4	1	7	2·1711	1·1
4	3	3	2·1699	66·8
5	1	2	2·1698	18·7
4	2	6	2·1546	7·1
2	2	10	2·1253	0·4
0	0	12	2·0967	15·0
4	0	8	2·0946	71·1

Isotypic compounds

For the series R_3Rh_2 with R = Gd, Tb, Dy, Ho, Er and Y, X-ray diffraction patterns of the alloy powders in the as-cast conditions were taken on a Guinier–de Wolff focusing camera with Cu $K\alpha$ radiation. In agreement with Ghassem & Raman (1973*b*), Gd_3Rh_2,

Table 4. *Lattice constants for* R_3Rh_2 *compounds with space group I*4/*mcm*

E.s.d.'s are in parentheses. V = volume of unit cell; n = number of atoms in the unit cell.

	a (Å)	c (Å)	$(V/n)^{1/3}$
Gd_3Rh_2	11·27 (1)	25·32 (2)	2·68
Tb_3Rh_2	11·25 (1)	25·20 (2)	2·67
Y_3Rh_2	11·232 (2)	25·16 (1)	2·66
Dy_3Rh_2	11·16 (1)	25·07 (2)	2·65
Ho_3Rh_2	11·11 (1)	24·99 (2)	2·64
Er_3Rh_2	11·09 (1)	24·88 (2)	2·63

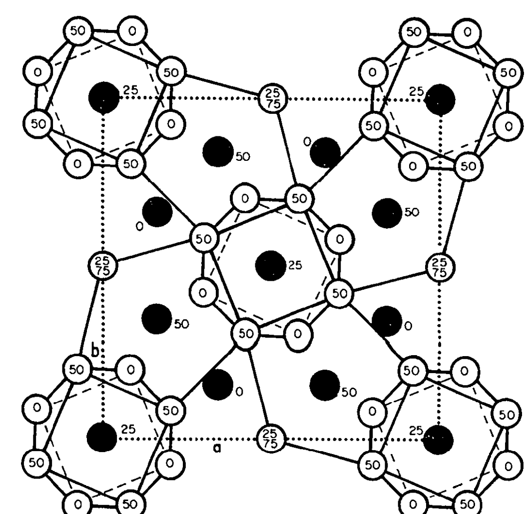

Fig. 1. Projection of the W_5Si_3 structure along **c** showing the Archimedian antiprisms around Si atoms at $z = 0{\cdot}25$ and the deformed pentagons around Si atoms at $z = 0{\cdot}50$. Black circles are Si atoms, open circles are W atoms. The numbers inscribed correspond to z parameters. The unit cell is dotted.

Tb_3Rh_2, Dy_3Rh_2 and Y_3Rh_2 have the same structure type as Er_3Rh_2. As expected we found Ho_3Rh_2 also isotypic with Er_3Rh_2. The parameters reported in Table 4 were obtained by least-squares refinement of reflexions measured from the films. The variation of the unit-cell parameters with the atomic number of the rare earth is a consequence of the normal lanthanide contraction.

Discussion

The structure of the R_3Rh_2 compounds presents a new type which has a resemblance to the W_5Si_3 structure type (Fig. 1). Layers of the Y_3Rh_2 structure are shown in projection along **c** in Fig. 2. It can be seen that the W_5Si_3 configuration and the layer of Y_3Rh_2 at $z_{Rh} \simeq \frac{1}{4}$

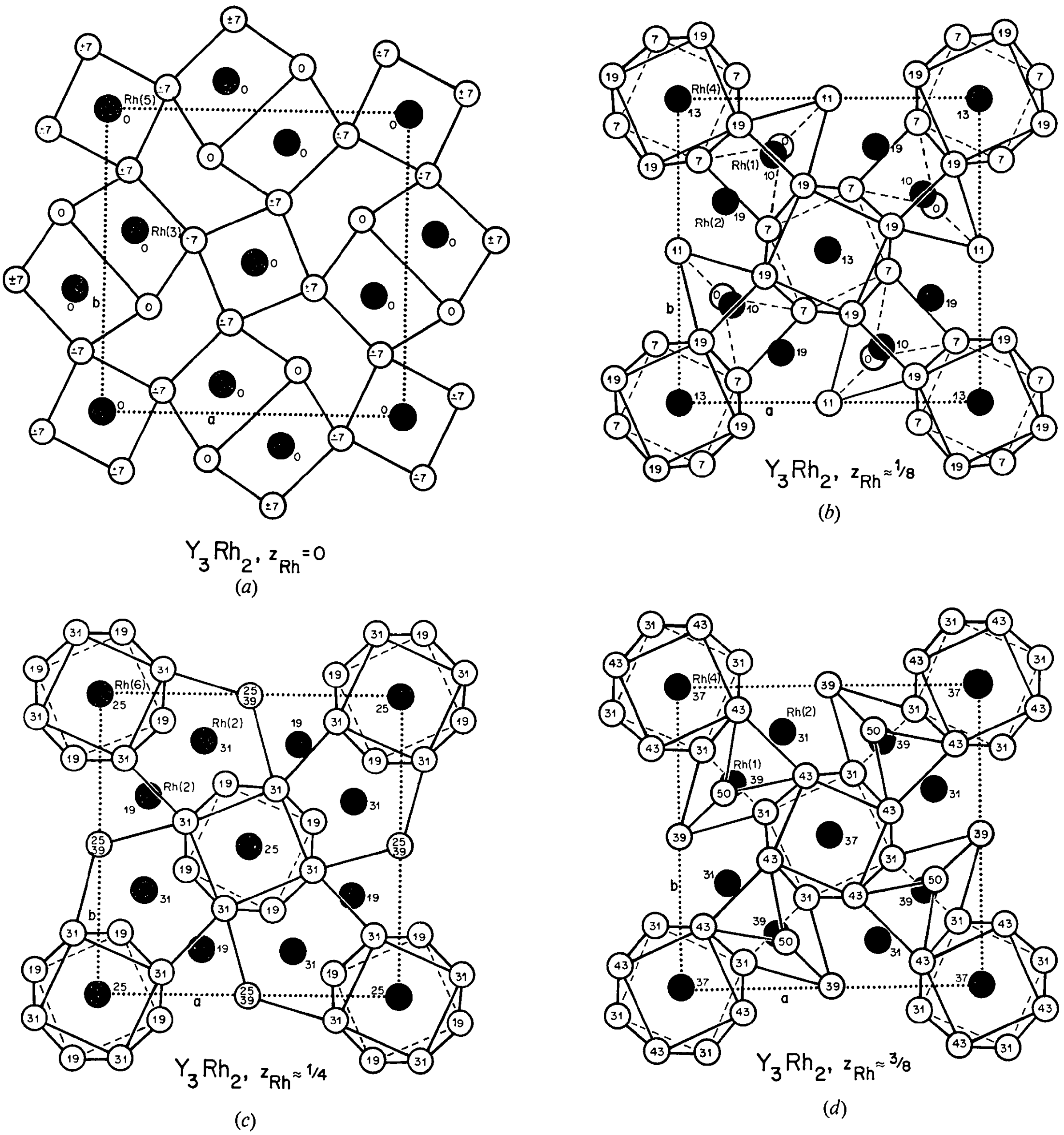

Fig. 2. The linkage of polyhedra around Rh atoms in Y_3Rh_2 shown in projection along **c**. Black circles are Rh atoms, open circles are Y atoms. The numbers inscribed correspond to z parameters. The unit cell is dotted. (*a*) Arrangement of cubes around Rh(5) at $z=0$ and trigonal prisms around Rh(3) at $z=0$. (*b*) Arrangement of Archimedian antiprisms around Rh(4) at $z=0{\cdot}13$ and trigonal prisms around Rh(1) at $z=0{\cdot}10$. (*c*) Arrangement of Archimedian antiprisms around Rh(6) at $z=0{\cdot}25$ and deformed pentagons around Rh(2) at $z=0{\cdot}31$. This arrangement is exactly the same as in W_5Si_3 (Fig. 1). (*d*) Arrangement of Archimedian antiprisms around Rh(4) at $z=0{\cdot}37$ and trigonal prisms around Rh(1) at $z=0{\cdot}39$.

(Fig. 2*c*) are identical. Layers at $z_{Rh} \simeq \frac{1}{8}$ (Fig. 2*b*) or $z_{Rh} \simeq \frac{3}{8}$ (Fig. 2*d*) show close similarities with W_5Si_3, but the layer at $z_{Rh}=0$ is completely different. Just as with the other rare-earth structures, a key to an understanding of this structure can be obtained from a precise analysis of the rare-earth polyhedra around the transition element atoms. A listing of interatomic distances around all Rh atoms in Y_3Rh_2 is given in Table 5. Rh(1) and Rh(3) are at the centre of a trigonal prism, Rh(4) and Rh(6) at the centre of an Archimedian antiprism and Rh(5) is at the centre of a cube. The coordination figure around Rh(2) is made up of six Y atoms and can be described by two equivalent figures: either a pentagon with one corner replaced by a pair of atoms along a direction perpendicular to the pentagon plane, or an Archimedian antiprism with two opposite corners through the centre of the antiprism missing. Coordination figures around all Rh atoms in Y_3Rh_2 are also shown in projection along **a** in Fig. 3.

Table 5. *Interatomic distances of* Rh *atoms in* Y_3Rh_2 *up to* 4 Å

All e.s.d.'s are less than 0·01 Å.

Rh(1)– Y(3)*	2·71 Å	Rh(4)–4Y(1)‡	2·91 Å
2Y(2)*	2·75	Rh(6)	2·93
Y(4)*	2·89	4Y(2)‡	2·95
2Y(1)*	2·90	Rh(5)	3·36
2Y(1)	3·27		
Rh(2)	3·34		
		Rh(5)–8 Y(1)§	3·03 Å
Rh(2)– Y(5)†	2·91 Å	2Rh(4)	3·36
2Y(2)†	3·04		
2Y(2)†	3·04		
Y(4)†	3·12	Rh(6)–8Y(2)‡	2·91 Å
Rh(1)	3·34	2Rh(4)	2·93
2Y(2)	3·43		
2Y(1)	3·46		
Rh(3)–2Y(3)*	2·85 Å		
4Y(1)*	2·88		
Rh(3)	3·05		
2Y(4)	3·21		

* Trigonal prism.
† Pentagon with one corner replaced by a pair of atoms perpendicular to pentagon plane.
‡ Archimedian antiprism.
§ Cube.

It appears useful therefore to review the type of rare-earth polyhedra which occur in binary compounds containing 50 or more R at.% in the R–Rh systems. Complete phase diagrams are known only for La–Rh (Singh & Raman, 1969), Nd–Rh (Singh & Raman, 1970) and Er–Rh (Ghassem & Raman, 1973*a*); however Ghassem & Raman (1973*b*) also studied parts of the phase equilibria and crystal structures in the Ce, Sm, Gd, Tb, Y and Dy–Rh systems. For compounds with more than 30 at.% Rh the lighter, bigger rare-earth elements form different structures than the heavier, smaller rare-earth elements. The structure types found are presented in Table 6.

Rare-earth rich compounds such as R_3Rh with Fe_3C structure type (Raman, 1972) and R_7Rh_3 with Th_7Fe_3 type (Olcese, 1973) are characterized by trigonal prisms of rare-earth atoms centred on Rh atoms. The kind of linkage of these trigonal prisms may be expressed by the trigonal prism linkage coefficient LC which can be obtained from the composition of the compound if the latter is rewritten as R_6Rh_{LC} (Moreau, Paccard & Parthé, 1976). For equiatomic compounds containing large rare-earth elements, the trigonal prism is also adopted. For example LaRh, CeRh, PrRh and NdRh crystallize with the CrB structure (Dwight, Conner & Downey, 1965). For compounds containing small rare-earth elements with more than 30 at.% Rh, the ability to form trigonal prisms is lost. Gd_5Rh_3, Tb_5Rh_3, Dy_5Rh_3 and Er_5Rh_3 crystallize with Mn_5Si_3 type (Raman & Ghassem, 1973) which has been shown to be characterized by deformed Si-centred Archimedian antiprisms (Parthé, Lux & Nowotny, 1955). Furthermore, the corresponding equiatomic compounds do not have trigonal prisms, but Rh-centred cubes instead. SmRh, GdRh, TbRh, DyRh, HoRh, ErRh, TmRh, LuRh and YRh crystallize with the CsCl structure

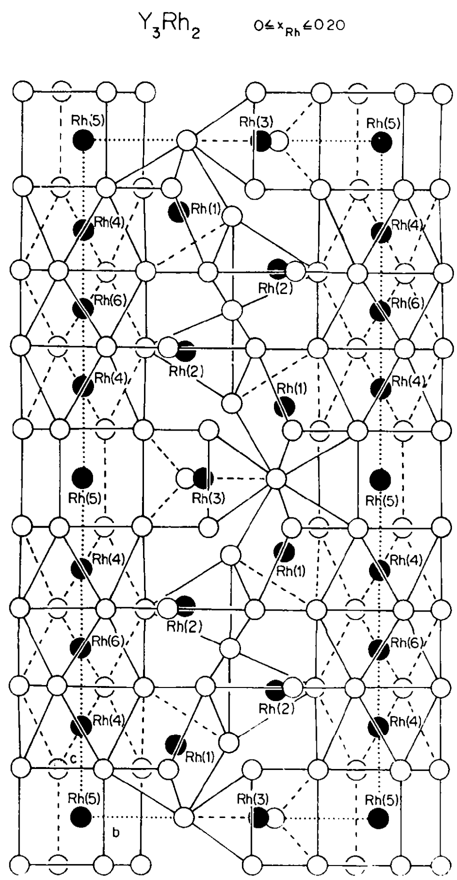

Fig. 3. The linkage of polyhedra around Rh atoms demonstrated in a projection along **a**. Black circles are Rh atoms and open circles are Y atoms. The unit cell is dotted.

Table 6. *Structure types found in* R–Rh *alloys* (*up to* 50 *at.*% Rh) *together with their characteristic rare-earth polyhedra*

Large R	Fe_3C Trigonal prisms	Th_7Fe_3 Trigonal prisms	La_5Rh_3 ?	Nd_4Rh_3 ?	CrB Trigonal prisms
Small R	Fe_3C Trigonal prisms	Th_7Fe_3 Trigonal prisms	Mn_5Si_3 Archimedian antiprisms	Y_3Rh_2 All types of polyhedra	CsCl Cubes

type (Dwight, Conner & Downey, 1965). The compounds with Y_3Rh_2 structure type occur with the small rare-earth elements from Gd to Er and thus the formation of a structure with only R_6Rh trigonal prisms seems unlikely. As shown above one finds all the different coordination polyhedra in Y_3Rh_2: trigonal prisms, Archimedian antiprisms and cubes.

References

ARONSSON, B. (1955). *Acta Chem. Scand.* **9**, 1107–1110.
CROMER, D. T. & MANN, J. B. (1968). *Acta Cryst.* A**24**, 321–324.
DWIGHT, A. E., CONNER, R. A. JR & DOWNEY, J. W. (1965). *Acta Cryst.* **18**, 835–839.
FLACK, H. D. (1974). *Acta Cryst.* A**30**, 569–573.
FLACK, H. D. (1975). *J. Appl. Cryst.* **8**, 520–521.
GHASSEM, H. & RAMAN, A. (1973*a*). *Metall. Trans.* **4**, 745–748.
GHASSEM, H. & RAMAN, A. (1973*b*). *Z. Metallk.* **64**, 197–199.
LARSON, A. C., ROOF, R. B. & CROMER, D. T. (1964). *Acta Cryst.* **17**, 1382–1386.
MOREAU, J. M., PACCARD, D. & PARTHÉ, E. (1974). *Acta Cryst.* B**30**, 2583–2586.
MOREAU, J. M., PACCARD, D. & PARTHÉ, E. (1976). *Acta Cryst.* B**32**, 496–500.
OLCESE, G. L. (1973). *J. Less-Common Met.* **33**, 71–81.
PARTHÉ, E., LUX, B. & NOWOTNY, H. (1955). *Mh. Chem.* **86**, 859–867.
RAMAN, A. (1972). *J. Less-Common Met.* **26**, 199–206.
RAMAN, A. & GHASSEM, H. (1973). *J. Less-Common Met.* **30**, 185–197.
SINGH, P. P. & RAMAN A. (1969). *Trans. AIME*, **245**, 1561–1568.
SINGH, P. P. & RAMAN, A. (1970). *Metall. Trans.* **1**, 233–237.
X-RAY system (1972). Version of June. Technical Report TR-192. Computer Science Center, Univ. of Maryland, College Park, Maryland.
YVON, K., JEITSCHKO, W. & PARTHÉ, E. (1969). *A Fortran* IV *Program for the Intensity Calculation of Powder Patterns*, 1969 *Version*. Laboratoire de Cristallographie aux Rayons X, Université de Genève, Switzerland.

Acta Cryst. (1976). B**32**, 1771

The Crystal Structure of the Antimony(III) Oxide Sulphate $Sb_6O_7(SO_4)_2$

BY JAN-OLOV BOVIN

Division of Inorganic Chemistry 2, *Chemical Center*, *University of Lund*, *P.O.B.* 740, *S*-220 07 *Lund*, *Sweden*

(*Received* 24 *November* 1975; *accepted* 31 *December* 1975)

The structure of $Sb_6O_7(SO_4)_2$ has been determined from intensities collected on a linear diffractometer with Mo $K\alpha$ radiation, and refined to an R of 0·041 for 1148 intensities. The crystals are orthorhombic, space group $Ccc2$, with $a=12·073$ (2), $b=19·023$ (4), $c=5·876$ (1) Å, $Z=4$. All three Sb^{III} atoms can be considered as three-coordinated and the coordination polyhedra are distorted tetrahedra, with the lone pair of electrons of Sb at one of the corners. The Sb–O distances within the tetrahedra vary between 1·994 (17) and 2·207 (18) Å. The three different SbO_3 polyhedra share corners and edges forming a cylindrical unit parallel to **c**. Each sulphate tetrahedron is situated between the cylindrical units.

Introduction

A compound of the composition $3Sb_2O_3.2SO_3$ has been reported to exist in equilibrium with 4·3–6·9M sulphuric acid solutions (Hintermann & Venuto, 1968). Contrary to this result the compound was earlier described as containing water, with composition $3Sb_2O_3.2SO_3.H_2O$ (Jander & Hartmann, 1965).

In nitric acid and perchloric acid solutions $Sb_4O_4(OH)_2(NO_3)_2$ and $Sb_4O_5(OH)ClO_4.\frac{1}{2}H_2O$ (Ahrland & Bovin, 1974) exist as stable phases. Both compounds contain distorted hexagonally close-packed sheets of Sb and O atoms (Bovin, 1974*a*, *b*, 1975). Earlier published structures of $SbPO_4$ (Kindberger, 1970) and $SbO(H_2PO_4).H_2O$ (Särnstrand, 1974), show however that, unlike the nitrate and perchlorate, these compounds are not built up of sheets.

The aim of the present work was to determine whether any water or hydroxide group exists in Sb^{III} oxide sulphate and to find out if the structure shows